Knockdown of Nemo-like kinase promotes metastasis in non-small-cell lung cancer

CUI SHI[1*], LIQIN XU[1*], ZHIYUAN TANG[1], WEISHUAI ZHANG[1], YULIN WEI[2],
JUN NI[3], SHUWEN ZHANG[1] and JIAN FENG[1]

[1]Department of Respiratory Medicine, Affiliated Hospital of Nantong University; [2]Department of Respiratory Medicine,
The Sixth People's Hospital of Nantong; [3]Department of Rehabilitation Medicine,
Affiliated Hospital of Nantong University, Nantong, Jiangsu 226001, P.R. China

Abstract. The evolutionarily conserved serine/threonine kinase Nemo-like kinase (NLK) serves an important role in cell proliferation, migration, invasion and apoptosis by regulating transcription factors among various cancers. In the present study, the function of NLK in human non-small cell lung cancer (NSCLC) was investigated. Immunohistochemical analysis and western blotting demonstrated that NLK expression was significantly reduced in NSCLC tissues compared with corresponding peritumoral tissues. Statistical analysis revealed that decreased NLK expression was associated with the presence of primary tumors, tumor node metastasis (TNM) staging, differentiation, lymph node metastasis, and E-cadherin and vimentin expression. Univariate analysis indicated that NLK expression, differentiation, lymph node metastasis, TNM stage, and E-cadherin and vimentin expression affected the prognosis of NSCLC. Cox regression analyses revealed NLK expression and TNM as independent factors that affected prognosis. Kaplan-Meier survival analysis revealed that patients with NSCLC and low NLK expression had relatively shorter durations of overall survival. *In vitro*, NLK overexpression inhibited A549 ncell migration and invasion as

Correspondence to: Dr Jian Feng, Department of Respiratory Medicine, Affiliated Hospital of Nantong University, Nantong, Jiangsu 226001, P.R. China
E-mail: jfeng68@126.com

*Contributed equally

determined by wound healing and Transwell migration assays, respectively. Additionally, immunofluorescence staining indicated that downregulation of NLK expression could induce epithelial-mesenchymal transition in NSCLC. NLK knockdown significantly decreased the expression of the epithelial marker E-cadherin, and markedly increased that of β-catenin and the mesenchymal marker vimentin. Furthermore, NLK was reported to directly interact with β-catenin as determined by a co-immunoprecipitation assay. Collectively, the results of the present study indicated that decreased NLK expression could promote tumor metastasis in NSCLC.

Introduction

Lung cancer is the leading cause of cancer-associated mortality among males, and has recently surpassed breast cancer as the most common cause of cancer-associated mortality among females (1). Histologically, human lung cancers can be categorized into small-cell lung cancer (SCLC) and non-SCLC (NSCLC). NSCLC comprises ~80% of all lung cancer cases, and mainly constitutes adenocarcinomas and squamous cell carcinomas (2). Notable reductions in smoking, and advances in early detection and treatment have been reported; however, the 5-year survival rate of patients with NSCLC is ≤18%. This is mainly due to the majority of patients that are diagnosed at advanced and later stages of cancer, and following the occurrence of metastasis (1). Therefore, understanding the molecular mechanisms that underlie the metastasis of NSCLC is necessary for the development of diagnostic technologies and novel treatment methods. Tumor metastasis is a complicated process involving numerous steps. The initial and most critical stage of metastasis includes the detachment of malignant cells from the primary tumor and invasion for the formation of a new lesion (3). Cancer cells promote their invasive potential by undergoing a phenotypic conversion referred to as the epithelial-mesenchymal transition (EMT), in which epithelial cells lose polarity and their cell-cell adhesion ability, acquiring a mesenchymal phenotype. This process involves a variety of signaling pathways and is dominated by several transcription factors (4,5). The numerous signaling pathways participating in this transition involve transforming growth factor β (TGFβ), bone

morphogenetic protein, Wnt/β-catenin, Notch, Hedgehog and receptor tyrosine kinases (6). In particular, activation of the Wnt/β-catenin signaling pathway was reported to promote EMT in various tumors (7).

Nemo-like kinase (NLK), initially identified as the photosensitive cluster required for the rotation of cells during *Drosophila* eye development, is an evolutionarily conserved mitogen-activated protein kinase (MAPK)-associated kinase (8). As a serine/threonine protein kinase that serves as an important negative regulatory molecule in the Wnt/β-catenin signaling pathway (9,10), NLK phosphorylates T cell factor/lymphoid enhancer factor proteins, inhibiting their binding to transcriptional response elements (11). Accumulating evidence has demonstrated that NLK serves a pivotal role in cell proliferation, migration, invasion and apoptosis via regulation of a variety of transcription components. For example, in human breast cancer cells, NLK was reported to associate with heat shock protein in the inhibition of apoptosis (12). NLK was revealed to also negatively regulate glioblastoma, in part via the inhibition of Wnt/β-catenin signaling (13). Additionally, NLK-mediated phosphorylation of histone deacetylase 1 was revealed to negatively regulate Wnt/β-catenin signaling to prevent the aberrant proliferation of non-transformed primary fibroblast cells (14). In addition, the negative modulation of the Wnt/β-catenin signaling pathway suppressed the progression of NSCLC (15). Therefore, it was proposed that NLK interacts with β-catenin in modulating EMT in NSCLC.

In the present study, the expression of NLK was analyzed via immunohistochemistry (IHC) and western blotting of fresh-frozen NSCLC tissue samples, and NSCLC tissue microarrays (TMAs). In addition, the association between NLK expression and the clinicopathological features of NSCLC, and the effects of altering NLK expression on NSCLC metastasis were determined. Furthermore, immunofluorescence staining and a co-immunoprecipitation assay were conducted to investigate the underlying mechanism.

Materials and methods

Sections and tissue samples. The present study included 159 NSCLC patients who had consented and enrolled before surgery (30 women and 121 men). Patient ages ranged from 39-83 years (median, 63.2 years). A total of 151 NSCLC sections for immunohistochemical analysis were obtained from patients with newly diagnosed NSCLC between 2005-2009, along with corresponding clinicopathological data. Eight fresh NSCLC samples and corresponding para-cancerous tissues from patients who underwent surgery but had received no chemotherapy or radiation therapy before sample collection were also collected for western blotting analysis between 2015-2016. All samples were collected at the Affiliated Hospital of Nantong University, Jiangsu Province, China. The study protocol was approved by the Human Research Ethics Committee of the Affiliated Hospital of Nantong University (Nantong, China). The collection of fresh-frozen human NSCLC tissue samples met the requirement of an institutional review board protocol approved by the Partners Human Research Committee Affiliated Hospital of Nantong University, Nantong, China). All tissue sections used for immunohistochemistry were formalin-fixed, and paraffin-embedded. Tumor staging was

in accordance with the guidelines of the 7th edition of TNM staging in lung cancer (16). The 5-year actual overall survival time was calculated from the date of surgery until the date of death or last follow-up appointment. Representative 2.0-mm tissue core samples from each patient were used to conduct TMA analysis (Shanghai Outdo Biotech Co., Ltd.). All tissues for immunoblot analysis were frozen immediately after surgery, then manually homogenized with a homogenizer in RIPA lysis buffer (cat. no. P0013B; Beyotime Institute of Biotechnology, Nantong, China). After centrifugation at 10,000 x g, 4°C for 15 min, the supernatant was extracted immediately for western blot analysis or stored at -80°C.

Immunohistochemistry (IHC). Immunostaining was performed using the avidin-biotin-peroxidase complex. Tissue sections were deparaffinized using a graded ethanol series, and endogenous peroxidase activity was blocked by soaking in 3% hydrogen peroxide (H_2O_2) for 10 min. The sections were then processed in 10 mmol/l citrate buffer (pH 6.0) and heated to 121°C in an autoclave for 20 min to retrieve the antigen. After rinsing in PBS (pH 7.2), the sections were incubated with anti-NLK (diluted 1:1,00; cat. no. ab116715) and anti-vimentin antibodies (diluted 1:1,00; cat. no. ab92547; both from Abcam) for 1 h at room temperature. All slides were processed using the peroxidase-anti-peroxidase method (Dako, Hamburg, Germany). After being rinsed in PBS, the peroxidase reaction was visualized by incubating the sections with a liquid mixture (0.02% diaminobenzidine tetrahydrochloride, 0.1% phosphate buffer solution, and 3% H_2O_2). After rinsing in water, the sections were counterstained with hematoxylin, dehydrated, and cover-slipped. Stained sections were observed under a microscope. The extent of immunostaining was evaluated and scored separately by two independent investigators with no prior knowledge of the clinical or pathological parameters of the patients. This TMA followed the Tissue Microarray System Quick-Ray manual (UT06; Unitma Co., Ltd.). For the semi-quantification of positive staining, both the intensity (0,1,2 or 3) and proportion of positive cells (0 to 100) were noted. Thus, the score ranged from 0 (no. staining) to 300 (all cells strongly stained). X-tile software (Rimm Laboratory, Yale University; http://www.tissuearray.org/rimmlab) (17) was used to divide the protein expression into two categories (low expression and high expression); high expression represented a microscopic score of 70-300, and low expression was from 0-70.

Western blotting. Tissues and cell protein were promptly homogenized after collection in a homogenization buffer containing 50 mM Tris-HCl, pH 7.5, 150 mM NaCl, 0.1% NP-40, 5 mM EDTA, 60 mM β-glycerophosphate, 0.1 mM sodium orthovanadate, 0.1 mM NaF, and complete protease inhibitor cocktail (Roche Diagnostics), then centrifuged at 12,000 x g for 15 min to collect the supernatant. Protein concentrations were measured with a BioRad protein assay (BioRad Laboratories, Inc.). The supernatant was diluted in 2X SDS loading buffer and boiled for 15 min. Proteins were then separated with 10% SDS-polyacrylamide gel electrophoresis, and transferred to polyvinylidene difluoride filter membranes (EMD Millipore). Then, the mass of protein loaded per lane was initially set at 200 μg, and the loading amount was adjusted according to the measured protein concentration.

The membranes were blocked with 5% non-fat milk in TBST (150 mM NaCl, 20 mM Tris, 0.05% Tween-20) for 2 h at room temperature. They were then washed three times with TBST and incubated overnight with primary antibodies anti-β-actin (dilution 1:500, cat. no. 4970, Cell Signaling Technology, Inc.), anti-NLK (dilution 1:500; cat. no. ab116715), anti-β-catenin (dilution 1:500; cat. no. ab22656), anti-E-cadherin (dilution 1:500; cat. no. ab1416), and anti-vimentin (dilution 1:500; cat. no. ab92547; all from Abcam). Horseradish peroxidase-linked IgG secondary antibodies (cat. no. A0208; Beyotime Institute of Biotechnology) at 1:5,000 dilution were added for 1 h incubation at room temperature. The band intensity was measured by the ImageJ analysis system (National Institutes of Health, USA) (18) and normalized against β-actin levels. Experiments were carried out on three separate occasions.

Cell cultures and transfection. The human NSCLC cell lines NCI-H1975, NCI-H1299, NCI-H1650, and A549 were purchased from the Shanghai Institute of Cell Biology Academia Sinica. All cancer cell lines were grown in RPMI-1640 medium supplemented with 10% fetal bovine serum, and 100 U/ml penicillin-streptomycin (Gibco-BRL; Thermo Fsiher Scientific, Inc.) at 37°C and 5% CO_2. The medium was changed after 24 h and replaced with fresh medium for transfection. Full-length NLK (Gene ID: 51701) was isolated from the human cDNA library. NLK-shRNA and control-shRNA lentiviruses were obtained from GeneChem Technologies. The shRNA target sequences were: 5'-GAATATCCGCTAAGGATGC-3' and 5'-CAGATCCAAGAGATGGAAA-3'. A549 cells were infected with control-shRNA or NLK-shRNA lentiviruses according to the manufacturer's protocol.

Wound healing assay. A549 cells were seeded in 6-well plates (Corning, Inc.) and transfected with NLK-shRNA, control-shRNA and full-length NLK according to the manufacturer's instructions (19). When they reached ~80% confluency 48 h post-transfection, cells were serum-starved for 12 h, then scratched using the fine end of a 100-μl pipette tip. Wound healing was observed at different time-points within the scrape line. Representative scrape line images were captured using an inverted Leica phase contrast microscope (Leica DFC 300 FX) under a 20x objective lens every 24 h. Image Processing and Analysis in Java was used to measure the wound healing assays. Duplicate wells for each condition were examined, and each experiment was repeated three times.

Invasion assay. The cell invasion assay was performed in a Transwell chamber (24-well type, 8 μm pore size; Corning, Inc.) with the BD Matrigel Basement Membrane Matrix according to the manufacturer's recommended protocol. Serum-free RPMI-1640 medium (0.5 ml) was placed in the upper chamber, and DMEM with 10% FBS was added to the bottom chambers. An equal amount ($1x10^5$) of cells were plated in the upper chambers of the quadruplicate wells and incubated at 37°C for 72 h. Cells were then fixed with methanol and stained with 3% crystal violet at 37°C to visualize the nuclei. The results of three independent experiments were averaged. Image Processing and Analysis in Java was used to assess the Transwell assay.

Immunofluorescence staining. Cells were seeded on coverslips in 24-well plates and cultured overnight. They were then washed with PBS, fixed with 4% paraformaldehyde for 1 h, and incubated at 4°C overnight with anti-β-catenin (dilution 1:100; cat. no. ab32572) and anti-vimentin (dilution 1:100; cat. no. ab92547; both from Abcam) antibodies. After three washes with PBS, the cells were incubated with Alexa Fluor-conjugated secondary antibodies (Alexa Fluor 594 (cat. no. R37117; dilution 1:200), Alexa Fluor 488 (cat. no. R37114; dilution 1:500; Molecular Probe, Inc.), and counterstained with DAPI. Fluorescence was detected using a Leica fluorescence microscope (Leica Microsystems GmbH). All assays were performed three times.

Co-immunoprecipitation. Immunoprecipitation was performed as previously described (20). Briefly, total cell lysates were incubated with an anti-NLK antibody, anti-β-catenin antibody or control IgG at 4°C overnight. Protein A/G (Sigma-Aldrich; Merck KGaA) was then added for 2 h at 4°C with gentle shaking. The precipitates were washed three times with homogenization buffer and boiled for another 15 min with SDS sample buffer followed by western blotting.

Statistical analyses. Values are presented as the means ± standard deviations (SDs) (21). Each experiment was repeated at least three times per condition. The Chi-square method was used to determine statistical significance. One-way analysis of variance (ANOVA) followed by Bonferroni post hoc test was used for the comparison of multiple groups. And SPSS 20.0 statistical software (IBM Corp.) was used for statistical analysis. Survival analysis was performed using the Kaplan-Meier method with the log-rank test. Univariate and multivariate analyses were based on the Cox proportional hazards regression model. A P-value <0.05 was considered statistically significant for all analyses.

Results

Expression of NLK in NSCLC tissues. To investigate the expression of NLK, E-cadherin and vimentin protein in NSCLC tissues, western blotting was performed in 8 pairs of fresh NSCLC and non-tumorous adjacent tissues. As presented in Fig. 1A and B, the expression levels of NLK and E-cadherin protein were significantly decreased in tumor tissues, while vimentin was upregulated compared with matched healthy tissues (P<0.05).

To further determine the association between NLK, E-cadherin and vimentin in NSCLC tissues, IHC analysis of 151 NSCLC patient samples was conducted. NLK was observed to be expressed mainly in the membrane and cytoplasm, E-cadherin was located in the membrane and vimentin was detected in the cytoplasm. NLK and E-cadherin were notably upregulated, while vimentin expression was decreased in healthy lung tissues compared with NSCLC tissues (Fig. 1C).

Analysis of the association between NLK and the clinicopathological features of NSCLC by TMA-IHC. Statistical analysis was performed to determine the association between NLK and the clinicopathological features of NSCLC (Table I) in 151 NSCLC specimens. A total of 89 (58.9%) patients exhibited
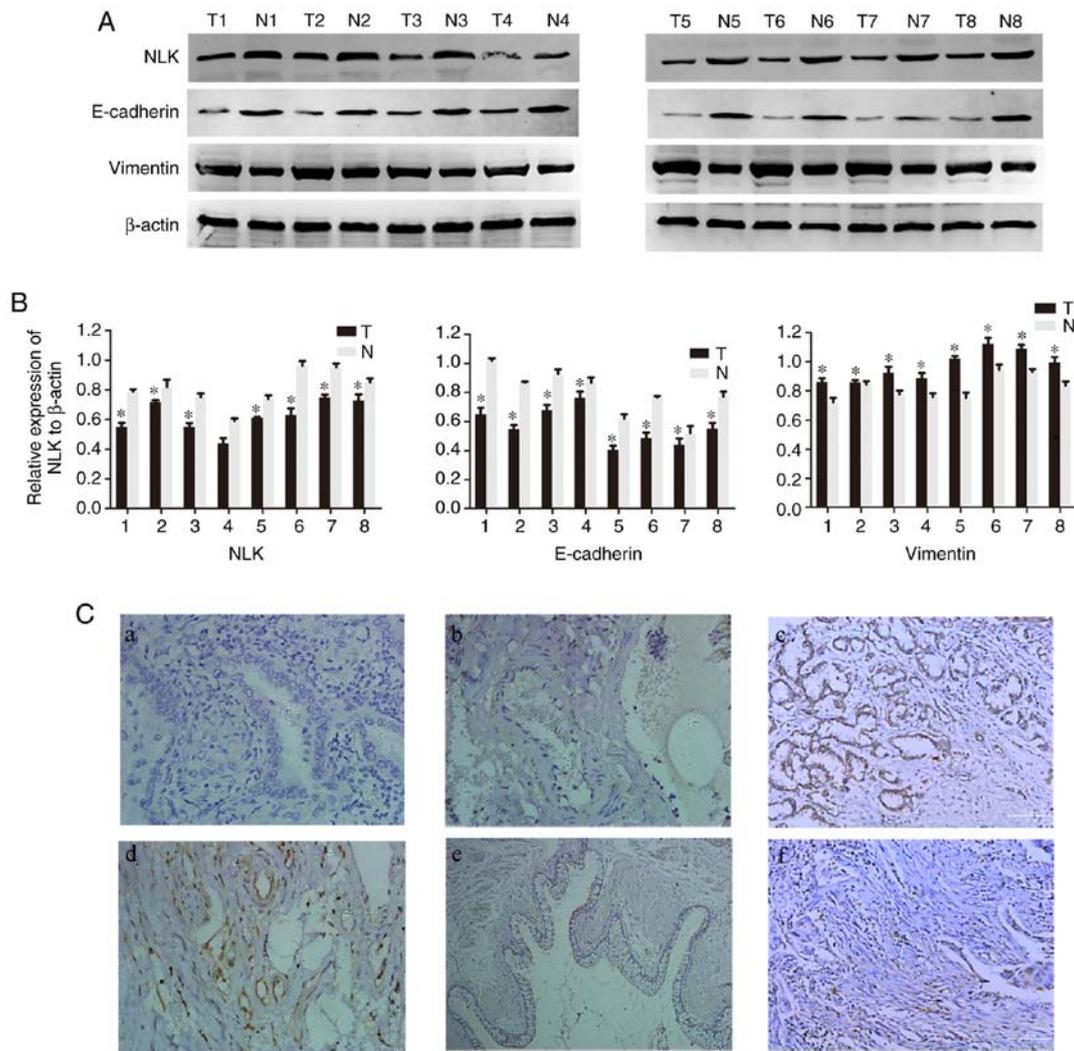
Figure 1. NLK expression is decreased in NSCLC tissues compared with adjacent non-tumorous tissues. (A) Western blotting revealed the downregulation of NLK expression in eight pairs of NSCLC tissues (T) compared with adjacent peritumoral tissues (N) β-actin was used as a loading control. (B) Histogram demonstrating the expression levels of NLK relative to β-actin by densitometry. Data are expressed as the means ± SD (*P<0.05, compared with adjacent tumor tissues). Experiments were repeated at least three times. (C) Immunohistochemical staining of NLK in NSCLC tissues. a and d, NLK expression; (b and e) E-cadherin expression; (c and f) vimentin expression. (a-c) NSCLC tissue samples. (d-f) healthy adjacent tissues. Magnification, x200. NLK, Nemo-like kinase; NSCLC, non-small cell lung cancer.

low or undetectable expression of NLK, while 62 (41.1%) presented NLK upregulation. NLK was significantly associated with TNM stage grouping (χ^2=7.885, P=0.019), primary tumor (χ^2=8.966, P=0.011), lymph node metastasis (χ^2=19.085, P<0.001), and E-cadherin (χ^2=47.111, P=0.001) and vimentin expression (χ^2=52.847, P<0.001). A notable association was observed between NLK expression and patient age, sex, smoking status, tumor size and histological type.

Survival analysis. A Cox proportional hazards model was constructed to perform univariate and multivariate analyses of all prognostic variables for the 5-year survival rate of patients with NSCLC (Table II). Univariate Cox regression analyses revealed that low NLK expression [hazard ratio (HR) 0.341, 95% confidence interval (CI) 0.219-0.531, P<0.001], lymph node metastasis (HR=5.732, 95% CI=3.732-8.803, P<0.001), advanced TNM stage (HR=3.214, 95% CI=2.341-3.941, P<0.001), and E-cadherin (HR=0.239, 95% CI=0.158-0.363, P<0.001) and vimentin expression (HR=5.820, 95%

CI=3.644-9.295, P<0.001) were significantly associated with the survival of patients with NSCLC for all variables. In addition, multivariate analysis indicated NLK expression (HR=0.387, 95% CI=0.248-0.605, P<0.001) and TNM (HR=3.037, 95% CI=2.341-3.941, P<0.001) as independent prognostic factors in patients with NSCLC. Collectively, the results inidcated that reduced expression of NLK could be a potential indicator of poor prognosis in NSCLC.

Kaplan-Meier survival curves further confirmed that the reduction of NLK protein expression was significantly associated with poor prognosis in patients with NSCLC (log-rank test, P<0.001; Fig. 2A). In accordance with NLK expression, the survival curve demonstrated a high degree of discrimination, indicating that the score standard for assessing NLK staining was suitable and that NLK was a reliable prognostic factor. Kaplan-Meier analysis also revealed that patients with lymph node metastasis had lower overall survival rates than patients without metastasis (log-rank test, P<0.001; Fig. 2B). Additionally, patients with lymph node metastasis and upregulated NLK

Table I. Correlation of NLK expression in tumorous tissues with clinicopathological characteristics in NSCLC patients.

Clinicopathological characteristics	n	NLK		Pearson χ^2	P-value
		Low or no expression	High expression		
Total	151	89	62		
Age at diagnosis (years)				0.663	0.416
<60	48	26 (54.2)	22 (45.8)		
≥60	103	63 (61.2)	40 (38.2)		
Sex				0.299	0.585
Male	121	70 (57.9)	51 (42.1)		
Female	30	19 (63.3)	11 (36.7)		
Smoking				6.785	0.376
Yes	57	31 (54.4)	26 (45.6)		
No	94	58 (61.7)	36 (38.3)		
Histopathology grading				2.118	0.347
Adenocarcinoma	97	53 (54.6)	44 (45.4)		
Squamous cell carcinoma	40	27 (67.5)	13 (32.5)		
Others	14	9 (64.3)	5 (35.7)		
Primary tumor				8.966	0.011[a]
T1	55	41 (74.5)	14 (25.5)		
T2	76	39 (51.3)	37 (48.77)		
T3+T4	20	9 (45)	11 (55)		
Stage grouping with TNM				7.885	0.019[a]
I	52	25 (48.1)	27 (51.9)		
II	57	32 (56.1)	25 (43.9)		
III	42	32 (76.2)	10 (23.8)		
Differentiation				6.896	0.032[a]
Low grade	43	20 (46.5)	23 (53.5)		
Middle grade	95	58 (61.1)	37 (38.9)		
High grade	13	11 (84.6)	2 (15.4)		
Lymph node metastasis				19.085	<0.001[a]
Yes	66	52 (78.8)	14 (21.2)		
No	85	37 (43.5)	48 (56.5)		
E-cadherin expression				47.111	<0.001[a]
Low	82	69 (84.1)	13 (15.9)		
High	69	20 (29.0)	49 (71.0)		
Vimentin expression				52.847	<0.001[a]
Low	64	16 (25.0)	48 (75.0)		
High	87	73 (83.9)	14 (16.1)		

Statistical analyses were performed by the Pearson Chi-square test. [a]P<0.05 was considered to indicate a statistically significant difference.

expression demonstrated significantly better prognosis than those with lymph node metastasis and downregulated NLK expression (P<0.05; Fig. 2B). Patients with increased NLK expression and no metastasis had a significantly higher overall survival rate than those with downregulated NLK expression and no metastasis (P=0.007; Fig. 2D).

Expression of NLK in NSCLC cell lines. To investigate the function of NLK in the carcinogenesis of NSCLC, NLK expression was determined in four NSCLC cell lines. Western blotting demonstrated upregulated NLK expression in A549 cells and

downregulated NLK expression in H1650 cells compared with H1975 and H1299 and (Fig. 3A and C). Subsequently, cells were transfected with NLK-shRNAs to downregulate the expression of NLK. As presented in Fig. 3B and D, western blotting revealed notable reductions in NLK protein expression in cells transfected with NLK-shRNAs compared with non-transfected or control-shRNA-transfected cells. In addition, a Flag-NLK vector was constructed to overexpress NLK in A549 cells.

NLK inhibits the migration and invasion of NSCLC cell lines. In advanced stages of cancer or postoperative recurrence,

Table II. Univariate and multivariate analyses of overall survival in 151 NSCLC specimens.

Characteristics	Univariate analysis			Multivariate analysis		
	HR	P-value	95% CI	HR	P-value	95% CI
NLK expression High vs. low	0.341	<0.001[a]	0.219-0.531	0.387	<0.001[a]	0.248-0.605
Sex Male vs. female	0.848	0.507	0.521-1.380			
Age (years) ≤60 vs. >60	1.141	0.536	0.751-1.733			
Smoking Yes vs. no	0.878	0.507	0.597-1.290			
Histopathology grading Ad vs. Sq vs. others	1.124	0.397	0.857-1.475			
Differentiation Low vs. middle vs. high grade	0.841	0.049[a]	0.708-0.999			
Primary tumor T1 vs. T2 vs. T3+T4	1.118	0.431	0.847-1.476			
Lymph node metastasis Yes vs. no	5.732	<0.001[a]	3.732-8.803			
TNM stage I vs. II vs. III+IV	3.214	<0.001[a]	2.475-4.173	3.037	<0.001[a]	2.341-3.941
E-cadherin expression High vs. low	0.239	<0.001[a]	0.158-0.363			
Vimentin expression High vs. low	5.820	<0.001[a]	3.644-9.295			

Statistical analyses were performed using log-rank test. [a]P<0.05 was considered to indicate a statistically significant difference.

NSCLC can be characterized by increased metastatic potential. Therefore, wound healing and Transwell assays were performed to investigate whether NLK affects NSCLC cell migration and invasion. In the wound healing assay, it was observed that the migration ability of the NLK-Flag group was decreased compared with the control group. Conversely, cells transfected with NLK-shRNA exhibited increased metastatic potential compared with the negative group; the migration ability of the NLK-shRNA group was promoted by reducing the expression of NLK (Fig. 4A). Similarly, the Transwell assay revealed that upregulating the expression of NLK suppressed cell migration compared with the control and negative groups (Fig. 4B).

NLK interacts with β-catenin in regulating EMT. To determine whether NLK affects EMT in NSCLC cells, immunofluorescence staining was conducted. A549 cells were transfected with NLK-shRNA and Flag-NLK; alterations in the expression of EMT markers were then analyzed. As presented in Fig. 5A, upregulating NLK expression via a Flag-NLK vector resulted in increased expression of the epithelial marker E-cadherin in the cell membrane, while the expression of the mesenchymal marker vimentin was decreased in the cytoplasm. Following NLK downregulation by NLK-shRNA, E-cadherin expression was notably undetected in the cell membrane, while vimentin expression was upregulated in the cytoplasm.

Western blotting revealed that upregulation of NLK led to increased E-cadherin expression, while that of vimentin and β-catenin was downregulated. Similarly, the expression of vimentin and β-catenin was increased, while that of E-cadherin was decreased following NLK downregulation (Fig. 5B and C). Immunoprecipitation of A549 cell protein revealed that NLK could co-immunoprecipitate with an anti-β-catenin antibody, but not under control conditions, indicating a naturally occurring interaction between endogenous NLK and β-catenin *in vivo* and vice versa. Thus, this could be a novel mechanism underlying the role of the tumor suppressor gene NLK in the progression of NSCLC (Fig. 5D and E).

Discussion

Since there is a lack of specific clinical features in early stage NSCLC, patients may possess an advanced stage disease prior to definitive diagnosis. NSCLC often metastasizes to the brain, bone, adrenal gland or liver tissues, which limits the use of optimal surgical procedures, and can lead to treatment failure and tumor-associated mortality. The invasion-metastasis cascade is comprised of two key steps: i) The spread of cancer cells from the primary tumor to distant tissues; and ii) the development of micro-metastases from cells that migrate to distant organs (22). According to research statistics, distant
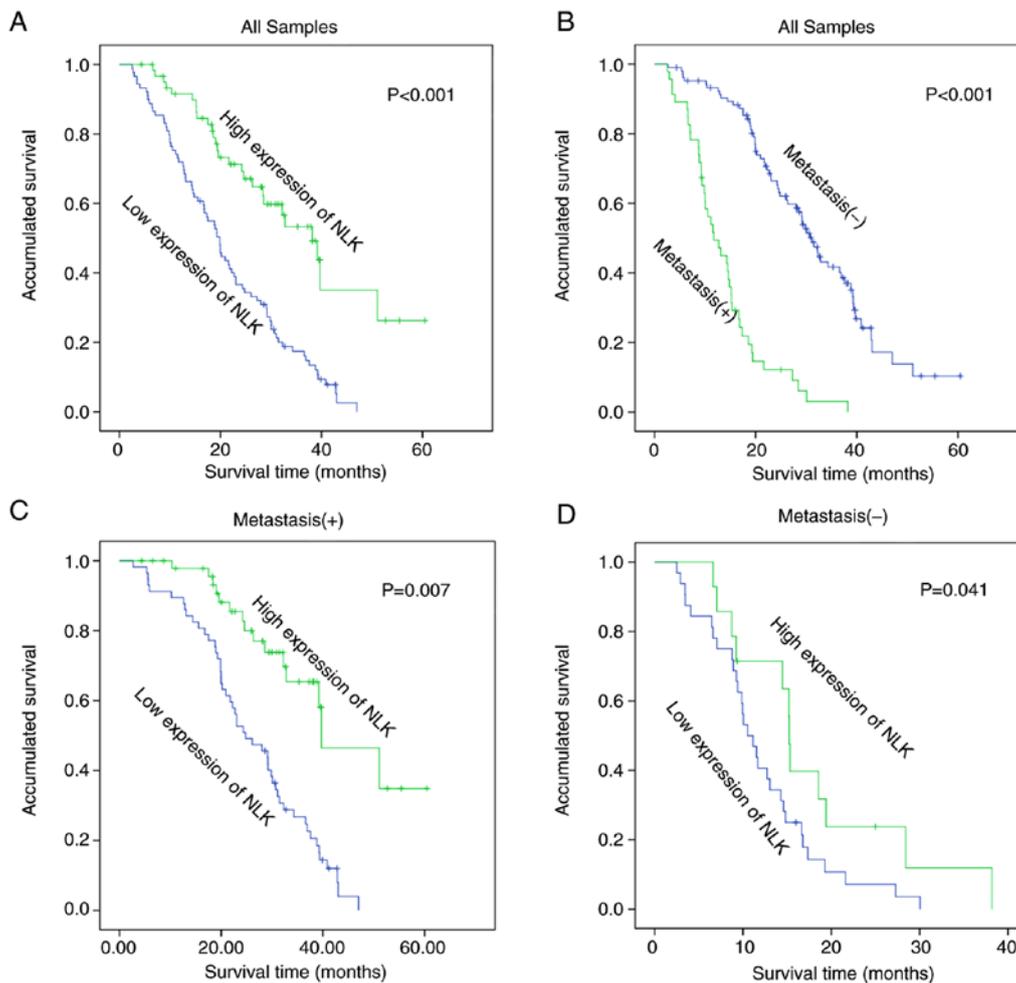
Figure 2. Association of NLK expression with overall survival in NSCLC patients by Kaplan-Meier analysis. (A) Patients with low NLK expression had shorter overall survival times. (B) Patients with metastasis had shorter overall survival times. (C and D) The association of NLK expression with poor prognosis in patients with and without metastasis. NLK, Nemo-like kinase; NSCLC, non-small cell lung cancer.

metastasis accounts for >90% of tumor-associated mortalities (23). Studies into the metastasis, survival and treatment of NSCLC have revealed that >50% of patients with NSCLC present with metastatic disease at the time of diagnosis, and only ~1% of patients survive for ≥5 years, with an intermediate survival of 7 months (24). Therefore, further investigation is required to determine the specific mechanism underlying NSCLC metastasis.

NLK was initially identified as a regulator of *Drosophila* photoreceptor development (8). NLK is an important member of the MAPK subfamily, and serves important roles in cell proliferation, invasion, metastasis, apoptosis and other biological processes. In the present study, 8 pairs of fresh NSCLC tissues and corresponding adjacent normal tissues were collected for immunoblotting, which demonstrated that NLK expression was significantly reduced in NSCLC tissues than corresponding adjacent normal tissues. To further analyze NLK expression in NSCLC tissues, paraffin-fixed samples from 151 patients with NSCLC were studied via IHC. The association between NLK expression and the clinicopathological features of NSCLC were statistically analyzed. The results demonstrated that NLK expression in NSCLC tissues was significantly decreased than in adjacent tissues, consistent with the findings from fresh tissues. Statistical analysis

revealed that low NLK expression was associated with pathological classification, clinical stage and lymph node metastasis in NSCLC. Cox multivariate regression analysis indicated low NLK expression as an independent factor affecting the prognosis of patients with NSCLC. Kaplan-Meier survival curves also indicated that the overall survival of patients with NSCLC and high NLK expression was significantly increased than those with low NLK expression. NLK may be involved in the pathophysiology of NSCLC. Emami *et al* (25) reported low NLK expression in prostate cancer, which could inhibit androgen receptor expression and promote the apoptosis of prostate cancer cells. Cui *et al* (26) reported that NLK expression in highly differentiated human glioblastoma was significantly lower than in poorly differentiated glioblastoma; the survival rate of patients with glioblastoma exhibiting low NLK expression was significantly increased than those with high expression levels. In nasopharyngeal carcinoma, calcium channel, voltage-dependent α 2/δ subunit 3 could induce mitochondrial-mediated apoptosis and activate NLK via the Wnt/Ca^{2+} pathway. This can antagonize Wnt signaling-mediated, anchorage-dependent and independent cell proliferation via cyclin D1 and CMYC, and respectively suppress invasion and EMT via matrix metalloproteinase 7 and snail family transcriptional repressor 1 (Snail) (27). These results indicated
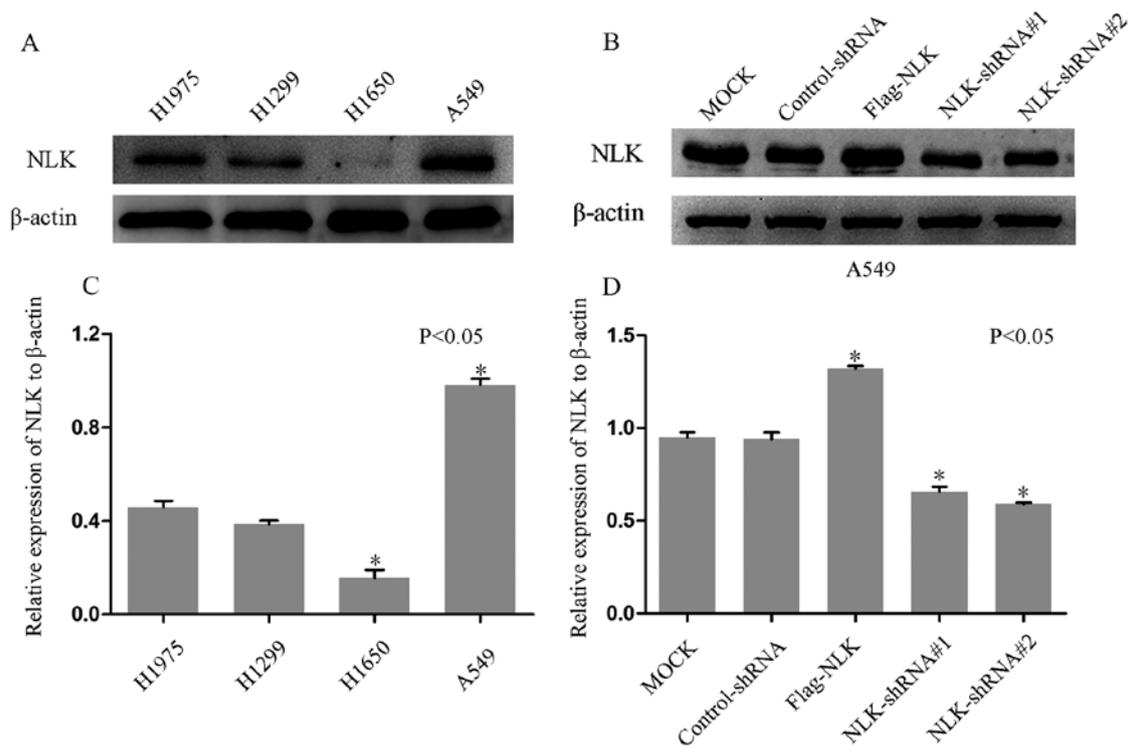
Figure 3. NLK expression in NSCLC cell lines. (A) NLK was expressed in the four NSCLC cell lines A549, H1299, H1975 and H1650 as demonstrated by western blotting. (B) Histogram demonstrating the expression levels of NLK in the four NSCLC cell lines A549, H1299, H1975 and H1650 as determined by densitometry. Data are expressed as the means ± SD (*P<0.05, compared with H1975 and H1299 cells). (C) Representative western blotting revealed the significant decrease in NLK expression following treatment of A549 cells with NLK-Flag, NLK-shRNA#1 and NLK-shRNA#2. (D) Histogram demonstrating the expression levels of NLK relative to β-actin by densitometry. Data are expressed as the means ± SD (*P<0.05 compared with control-shRNA). Experiments were repeated at least three times. NLK, Nemo-like kinase; NSCLC, non-small cell lung cancer.
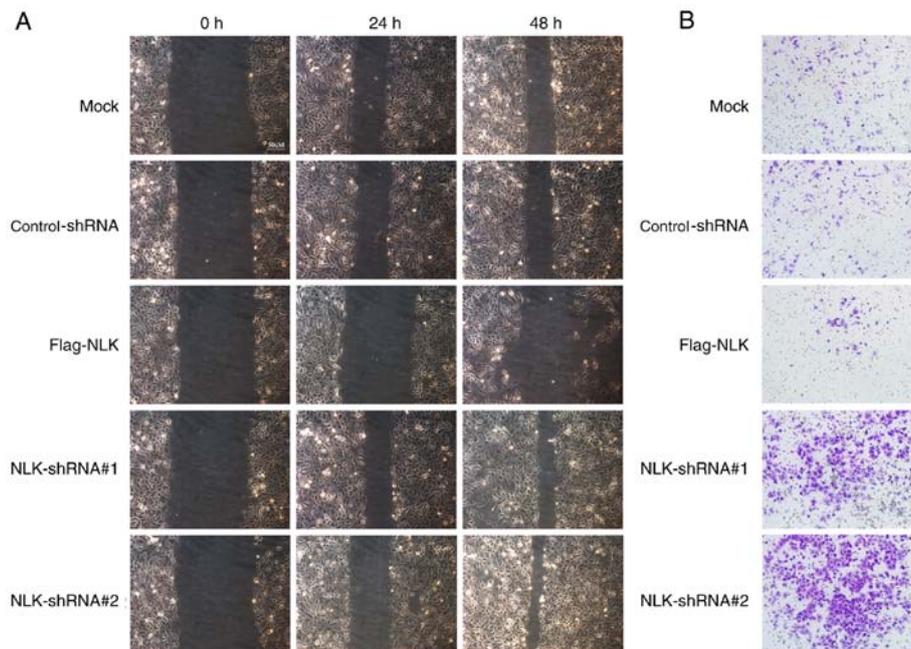
Figure 4. Wound healing assay and Transwell assay. (A) Migration of cells treated with shNLK, Flag-NLK, or negative control to the wound was visualized at 0, 24 and 48 h with an inverted Leica phase contrast microscope. (B) Invasion of cells treated with shNLK, Flag-NLK or negative control through the micropore membrane as visualized at 48 h. NLK, Nemo-like kinase.

that NLK may be a tumor suppressor in cell proliferation, EMT and tumor metastasis. Investigations into gallbladder cancer demonstrated that NLK was upregulated in cancer tissues, which was associated with the poor prognosis of patients (28). Notably, Lv *et al* reported that increased NLK expression in SCLC could promote invasion and metastasis (29). Conversely,

Figure 5. NLK interacts with β-catenin and regulates EMT in NSCLC. (A) A549 cells transfected with (a-c) Mock; (d-f) Control-shRNA; (g-i) NLK-Flag; (j-l) NLK-shRNA#1; and (m-o) NLK-shRNA#2 were fixed and processed for immunofluorescence with antibodies against β-catenin and vimentin. Results are obtained from three independent experiments. (B) Representative western blotting revealing that NLK expression in A549 cells was decreased by NLK-shRNA and upregulated by NLK-Flag. E-cadherin expression was consis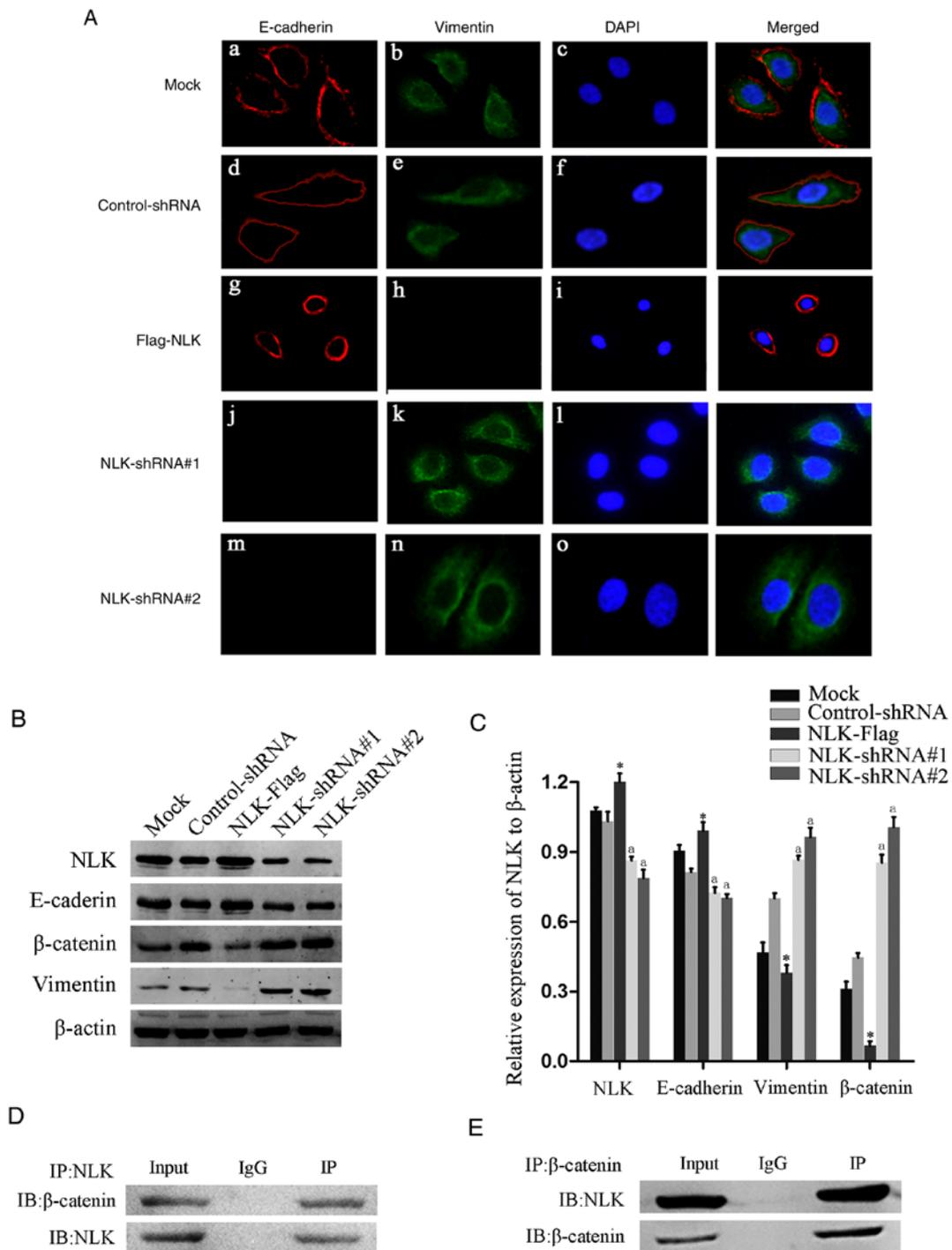tent with that of NLK, however, β-catenin, and vimentin expression revealed opposite expression levels. (C) Histogram demonstrating NLK expression levels relative to β-actin by densitometry. Data are expressed as the means ± SD (^{*,a}P<0.05 compared with control-shRNA). (D and E) Western blotting of NLK-β-catenin co-immunoprecipitation in A549 cells. NLK, Nemo-like kinase; EMT, epithelial-mesenchymal transition; NSCLC, non-small cell lung cancer,

the present study observed reduced NLK expression in NSCLC; this may reflect the differential expression of NLK in organs, tissues and the internal environment of cells (30).

The present study reported that the expression of E-cadherin in the NSCLC cell membrane was reduced, while that of vimentin was increased compared in normal tissue. Statistical analysis revealed that NLK expression was associated with

E-cadherin and vimentin. In addition, the expression of E-cadherin and vimentin in A549 cells following transfection was determined. Immunofluorescence analysis demonstrated that E-cadherin expression was significantly reduced, while that of vimentin was increased following NLK knockdown compared with the control group. Opposing findings were obtained when NLK was overexpressed in cells. This indicated

that NLK serves an important role in EMT, which is associated with tumor metastasis (31-35). In NSCLC, forkhead box Q1 could promote tumor metastasis by inducing EMT, leading to adverse prognosis (36). In colorectal cancer, Wnt can activate pre-B-cell leukemia transcription factor 3, and promote tumor proliferation and metastasis by inducing EMT via Snail and zinc finger E-box-binding homeobox 1 (37).

To determine the role of NLK in the metastasis of NSCLC, NLK expression and its effects on NSCLC invasion and metastasis were investigated at the cellular level. NLK expression was analyzed in four NSCLC cell lines via immunoblotting in the present study. A549 cells were selected for further analysis as these cells exhibited relatively higher NLK expression. Following the transfection of A549 cells with an NLK-overexpression plasmid, the expression of NLK increased significantly, and decreased after shRNA-mediated interference. The scratch-wound and Transwell assays demonstrated that the viability, and invasive and metastatic potentials of A549 cells transfected with the NLK-overexpression plasmid were significantly reduced than the control group. Conversely, the invasive and metastatic potentials of A549 cells transfected with NLK-shRNA were significantly promoted compared to the control group. Therefore, the present study proposed that NLK may serve a role in the metastatic process of NSCLC. In the past decade, a number of studies have reported that a quantity of transcription factors and co-factors have been demonstrated to be phosphorylated and regulated by NLK (38). Previous studies found that NLK participated in NSCLC cell proliferation by modulating the Wnt signaling pathway (5). Moreover, aberrant expression of NLK was correlated with proliferation and apoptosis in hepatocellular carcinoma (39), as well as prostate (25) and colon cancer (40). The present study revealed that NLK had impacts on metastasis of cells via regulation of EMT in NSCLC. As is recognized, EMT is closely related to tumor metastasis. Hence, the hypothesis that high-expression of NLK may inhibit NSCLC metastasis was put forward. However, it is still unclear whether the effects of NLK on proliferation and apoptosis are related to cell migration and invasion in NSCLC, this requires further study.

TGFβ, Wnt/β-catenin, nuclear factor-κB and Hedgehog serve important roles in regulating EMT. In several tumor models, the Wnt/β-catenin signaling pathway has been reported to regulate EMT (41-47). In oral squamous cell carcinoma, SRY-box 8 regulates stem cell-like protein and platinum-induced EMT by activating the Wnt/β-catenin signaling pathway. In breast cancer, microRNA-23a activates the Wnt/β-catenin signaling pathway via direct interaction with cadherin-1, and promotes TGFβ 1-induced EMT and tumor metastasis (43). Yang *et al* (7) and Liang *et al* (48) reported that Wnt/β-catenin promoted the metastasis of NSCLC by inducing EMT, and revealed that NLK antibodies could be used to form an NLK-interacting β-catenin immunoprecipitation complex. These protein complexes suggest that NLK may interact directly or indirectly with β-catenin. Therefore, low levels of NLK expression in NSCLC may induce EMT by regulating the Wnt/β-catenin signaling pathway.

In conclusion, NSCLC was reported to exhibit reduced NLK expression levels, which could be associated with metastasis and the poor prognosis of NSCLC. Dysregulating the expression of NLK in A549 cells significantly altered the invasive and migration potentials of tumor cells. In addition, NLK was proposed to be involved in EMT in NSCLC, and serve an important role in the Wnt/β-catenin signaling pathway in this process.

Availability of data and materials

The datasets used during the present study are available from the corresponding author upon reasonable request.

Authors' contributions

CS and LX completed most of the experimental part and the writing of the article. JF is the head of the project, responsible for the project design, normal operation and coordination of the project. The other co-authors participated in some experiments of this study. CS, JN, YW and SZ were responsible for collecting cases. JN and YW directed the experimental design and technical guidance for the immunofluorescence experiment, and they completed most of the related data analysis. ZT and WZ assisted CS and LX in molecular biology experiments.

Ethics approval and consent to participate

The study protocol was approved by the Human Research Ethics Committee of the Affiliated Hospital of Nantong University (Nantong, China) and patients provided consent and enrolled before surgery.

Patient consent for publication

Not applicable.

Competing interests

The authors declare that they have no competing interests.

References

1. Torre LA, Bray F, Siegel RL, Ferlay J, Lortet-Tieulent J and Jemal A: Global cancer statistics, 2012. CA Cancer J Clin 65: 87-108, 2015.
2. Siegel RL, Miller KD and Jemal A: Cancer statistics, 2017. CA Cancer J Clin 67: 7-30, 2017.
3. Fidler IJ: The pathogenesis of cancer metastasis: The 'seed and soil' hypothesis revisited. Nat Rev Cancer 3: 453-458, 2003.
4. Grunert S, Jechlinger M and Beug H: Diverse cellular and molecular mechanisms contribute to epithelial plasticity and metastasis. Nat Rev Mol Cell Biol 4: 657-665, 2003.
5. Bogenrieder T and Herlyn M: Axis of evil: Molecular mechanisms of cancer metastasis. Oncogene 22: 6524-6536, 2003.

6. Gonzalez DM and Medici D: Signaling mechanisms of the epithelial-mesenchymal transition. Sci Signal 7: re8, 2014.
7. Yang S, Liu Y, Li MY, Ng CSH, Yang SL, Wang S, Zou C, Dong Y, Du J, Long X, et al: FOXP3 promotes tumor growth and metastasis by activating Wnt/β-catenin signaling pathway and EMT in non-small cell lung cancer. Mol Cancer 16: 124, 2017.
8. Choi KW and Benzer S: Rotation of photoreceptor clusters in the developing Drosophila eye requires the nemo gene. Cell 78: 125-136, 1994.
9. Takada I, Mihara M, Suzawa M, Ohtake F, Kobayashi S, Igarashi M, Youn MY, Takeyama K, Nakamura T, Mezaki Y, et al: A histone lysine methyltransferase activated by non-canonical Wnt signalling suppresses PPAR-gamma transactivation. Nat Cell Biol 9: 1273-1285, 2007.
10. Ishitani T, Kishida S, Hyodo-Miura J, Ueno N, Yasuda J, Waterman M, Shibuya H, Moon RT, Ninomiya-Tsuji J and Matsumoto K: The TAK1-NLK mitogen-activated protein kinase cascade functions in the Wnt-5a/Ca(2+) pathway to antagonize Wnt/beta-catenin signaling. Mol Cell Biol 23: 131-139, 2003.
11. Yamada M, Ohnishi J, Ohkawara B, Iemura S, Satoh K, Hyodo-Miura J, Kawachi K, Natsume T and Shibuya H: NARF, an nemo-like kinase (NLK)-associated ring finger protein regulates the ubiquitylation and degradation of T cell factor/lymphoid enhancer factor (TCF/LEF). J Biol Chem 281: 20749-20760, 2006.
12. Shaw-Hallgren G, Chmielarska Masoumi K, Zarrizi R, Hellman U, Karlsson P, Helou K and Massoumi R: Association of nuclear-localized Nemo-like kinase with heat-shock protein 27 inhibits apoptosis in human breast cancer cells. PLoS One 9: e96506, 2014.
13. Sa JK, Yoon Y, Kim M, Kim Y, Cho HJ, Lee JK, Kim GS, Han S, Kim WJ, Shin YJ, et al: In vivo RNAi screen identifies NLK as a negative regulator of mesenchymal activity in glioblastoma. Oncotarget 6: 20145-20159, 2015.
14. Masoumi KC, Daams R, Sime W, Siino V, Ke H, Levander F and Massoumi R: NLK-mediated phosphorylation of HDAC1 negatively regulates Wnt signaling. Mol Biol Cell 28: 346-355, 2017.
15. Lv L, Wan C, Chen B, Li M, Liu Y, Ni T, Yang Y, Liu Y, Cong X, Mao G and Xue Q: Nemo-like kinase (NLK) inhibits the progression of NSCLC via negatively modulating WNT signaling pathway. J Cell Biochem 115: 81-92, 2014.
16. Goldstraw P, Chansky K, Crowley J, Rami-Porta R, Asamura H, Eberhardt WE, Nicholson AG, Groome P, Mitchell A, Bolejack V, et al: The IASLC lung cancer staging project: Proposals for revision of the TNM stage groupings in the forthcoming (Eighth) edition of the TNM classification for lung cancer. J Thorac Oncol 11: 39-51, 2016.
17. Zhai X, Xu L, Zhang S, Zhu H, Mao G and Huang J: High expression levels of MAGE-A9 are correlated with unfavorable survival in lung adenocarcinoma. Oncotarget 7: 4871-4881, 2016.
18. Tang Z, Li J, Shen Q, Feng J, Liu H, Wang W, Xu L, Shi G, Ye X, Ge M, et al: Contribution of upregulated dipeptidyl peptidase 9 (DPP9) in promoting tumoregenicity, metastasis and the prediction of poor prognosis in non-small cell lung cancer (NSCLC). Int J Cancer 140: 1620-1632, 2017.
19. Zhang J, Zhu J, Yang L, Guan C, Ni R, Wang Y, Ji L and Tian Y: Interaction with CCNH/CDK7 facilitates CtBP2 promoting esophageal squamous cell carcinoma (ESCC) metastasis via upregulating epithelial-mesenchymal transition (EMT) progression. Tumour Biol 36: 6701-6714, 2015.
20. Zhang S, Shi W, Chen Y, Xu Z, Zhu J, Zhang T, Huang W, Ni R, Lu C and Zhang X: Overexpression of SYF2 correlates with enhanced cell growth and poor prognosis in human hepatocellular carcinoma. Mol Cell Biochem 410: 1-9, 2015.
21. Xue Q, Lv L, Wan C, Chen B, Li M, Ni T, Liu Y, Liu Y, Cong X, Zhou Y, et al: Expression and clinical role of small glutamine-rich tetratricopeptide repeat (TPR)-containing protein alpha (SGTA) as a novel cell cycle protein in NSCLC. J Cancer Res Clin Oncol 139: 1539-1549, 2013.
22. Valastyan S and Weinberg RA: Tumor metastasis: Molecular insights and evolving paradigms. Cell 147: 275-292, 2011.
23. Chaffer CL and Weinberg RA: A perspective on cancer cell metastasis. Science 331: 1559-1564, 2011.
24. Lovly CM and Carbone DP: Lung cancer in 2010: One size does not fit all. Nat Rev Clin Oncol 8: 68-70, 2011.
25. Emami KH, Brown LG, Pitts TE, Sun X, Vessella RL and Corey E: Nemo-like kinase induces apoptosis and inhibits androgen receptor signaling in prostate cancer cells. Prostate 69: 1481-1492, 2009.
26. Cui G, Li Z, Shao B, Zhao L, Zhou Y, Lu T, Wang J, Shi X, Wang J, Zuo G, et al: Clinical and biological significance of nemo-like kinase expression in glioma. J Clin Neurosci 18: 271-275, 2011.
27. Zhang Y, Peng C, Wu G, Wang Y, Liu R, Yang S, He S, He F, Yuan Q, Huang Y, et al: Expression of NLK and its potential effect in ovarian cancer chemotherapy. Int J Gynecol Cancer 21: 1380-1387, 2011.
28. Li M, Zhang S, Wang Z Zhang B, Wu X, Weng H, Ding Q, Tan Z, Zhang N, Mu J, et al: Prognostic significance of nemo-like kinase (NLK) expression in patients with gallbladder cancer. Tumour Biol 34: 3995-4000, 2013.
29. Lv M, Li Y, Tian X, Dai S, Sun J, Jin G and Jiang S: Lentivirus-mediated knockdown of NLK inhibits small-cell lung cancer growth and metastasis. Drug Des Devel Ther 10: 3737-3746, 2016.
30. Ishitani T and Ishitani S: Nemo-like kinase, a multifaceted cell signaling regulator. Cell Signal 25: 190-197, 2013.
31. Brabletz T, Kalluri R, Nieto MA and Weinberg RA: EMT in cancer. Nat Rev Cancer 18: 128-134, 2018.
32. George JT, Jolly MK, Xu S, Somarelli JA and Levine H: Survival outcomes in cancer patients predicted by a partial EMT Gene expression scoring metric. Cancer Res 77: 6415-6428, 2017.
33. Duhamel S, Goyette MA, Thibault MP, Filion D, Gaboury L and Côté JF: The E3 ubiquitin ligase HectD1 suppresses EMT and metastasis by targeting the +TIP ACF7 for degradation. Cell Rep 22: 1016-1030, 2018.
34. Singh M, Yelle N, Venugopal C and Singh SK: EMT: Mechanisms and therapeutic implications. Pharmacol Ther 182: 80-94, 2018.
35. Nieto MA, Huang RY, Jackson RA and Thiery JP: EMT: 2016. Cell 166: 21-45, 2016.
36. Feng J, Zhang X, Zhu H, Wang X, Ni S and Huang J: FoxQ1 overexpression influences poor prognosis in non-small cell lung cancer, associates with the phenomenon of EMT. PLoS One 7: e39937, 2012.
37. Lamprecht S, Kaller M, Schmidt EM, Blaj C, Schiergens TS, Engel J, Jung A, Hermeking H, Grünewald TGP, Kirchner T, et al: PBX3 is part of an EMT regulatory network and indicates poor outcome in colorectal cancer. Clin Cancer Res 24: 1974-1986, 2018.
38. Kim S, Kim Y, Lee J and Chung J: Regulation of FOXO1 by TAK1-Nemo-like kinase pathway. J Biol Chem 285: 8122-8129, 2010.
39. Ishikawa T, Shimizu D, Kito A, Ota I, Sasaki T, Tanabe M, Yamada A, Arioka H, Shimizu S, Wakasugi J, et al: Breast cancer manifested by hematologic disorders. J Thorac Dis 4: 650-654, 2012.
40. Yasuda J, Tsuchiya A, Yamada T, Sakamoto M, Sekiya T and Hirohashi S: Nemo-like kinase induces apoptosis in DLD-1 human colon cancer cells. Biochem Biophys Res Commun 308: 227-233, 2003.
41. Xie SL, Fan S, Zhang SY, Chen WX, Li QX, Pan GK, Zhang HQ, Wang WW, Weng B, Zhang Z, et al: SOX8 regulates cancer stem-like properties and cisplatin-induced EMT in tongue squamous cell carcinoma by acting on the Wnt/β-catenin pathway. Int J Cancer 142: 1252-1265, 2018.
42. Ma F, Li W, Liu C, Li W, Yu H, Lei B, Ren Y, Li Z, Pang D and Qian C: MiR-23a promotes TGF-β1-induced EMT and tumor metastasis in breast cancer cells by directly targeting CDH1 and activating Wnt/β-catenin signaling. Oncotarget 8: 69538-69550, 2017.
43. Hu Y, Qi MF, Xu QL, Kong XY, Cai R, Chen QQ, Tang HY and Jiang W: Candidate tumor suppressor ZNF154 suppresses invasion and metastasis in NPC by inhibiting the EMT via Wnt/β-catenin signalling. Oncotarget 8: 85749-85758, 2017.
44. Guo YH, Wang LQ, Li B, Xu H, Yang JH, Zheng LS, Yu P, Zhou AD, Zhang Y, Xie SJ, et al: Wnt/β-catenin pathway transactivates microRNA-150 that promotes EMT of colorectal cancer cells by suppressing CREB signaling. Oncotarget 7: 42513-42526, 2016.
45. Liu X, Li Z, Song Y, Wang R, Han L, Wang Q, Jiang K, Kang C and Zhang Q: AURKA induces EMT by regulating histone modification through Wnt/β-catenin and PI3K/Akt signaling pathway in gastric cancer. Oncotarget 7: 33152-33164, 2016.
46. Gu Y, Wang Q, Guo K, Qin W, Liao W, Wang S, Ding Y and Lin J: TUSC3 promotes colorectal cancer progression and epithelial-mesenchymal transition (EMT) through WNT/β-catenin and MAPK signalling. J Pathol 239: 60-71, 2016.
47. Duan H, Yan Z, Chen W, Wu Y, Han J, Guo H and Qiao J: TET1 inhibits EMT of ovarian cancer cells through activating Wnt/β-catenin signaling inhibitors DKK1 and SFRP2. Gynecol Oncol 147: 408-417, 2017.
48. Liang Z, Lu L, Mao J, Li X, Qian H and Xu W: Curcumin reversed chronic tobacco smoke exposure induced urocystic EMT and acquisition of cancer stem cells properties via Wnt/β-catenin. Cell Death Dis 8: e3066, 2017.